Supporting Information

Androutsellis-Theotokis et al. 10.1073/pnas.0905125106

SI Text

Supplementary Methods. ***Cell culture.*** E13.5 neural stem cells were grown as previously described (1). Cells were expanded in serum-free DMEM/F12 medium with N2 supplement and FGF2 (20 ng/mL) for 5 days under 5% oxygen conditions and were replated fresh or from frozen stocks at 1,000–10,000 cells/cm^2. FGF2 was included throughout our experiments, unless otherwise stated. Adult rat (3–6 months old) or adult mouse (2–4 months old) SVZ neural stem cell (NSC) cultures were grown in the same medium as the fetal cultures.

Immunohistochemistry. Under deep anesthesia, animals were perfused transcardially with a rinse of saline, followed by 4% formaldehyde fixative (pH 7.4). Brains were removed immediately, stored in the fixative solution overnight, and then in 30% sucrose for 3 days. Brains were frozen-sectioned at 16 or 30 μm. Immunohistochemical detection of BrdU was performed with an antigen-retrieval step (sections were boiled in 0.02 M citrate, pH 6.0, in a microwave for 5 min, washed 3 times with PBS, and incubated for 45 min in 2 M HCl, at room temperature).

As expected from genetic studies, the Hes3 antibody recognized adult Purkinje cells in sections and protein extracts from the mouse cerebellum; it did not, however recognize proteins in extracts from Hes3 null cerebelli (Fig. S3*a* and *b*). Both fetal and adult NSC cultures express Hes3; expression is lost following differentiation by mitogen withdrawal (Fig. S4*c* and *d*). The anti-Tie2 antibodies have been independently validated by other laboratories (2, 3).

Rodent MRI Imaging. ***$MnCl_2$ administration.*** Adult male Sprague-Dawley rats received stereotactical injections of 6-OHDA into the right striatum, and saline injections of equal volume into the left striatum as a negative control. To use Mn^{2+} as a contrast agent (4–6), rats were injected i.p. with 30 mg/kg $MnCl_2$ 24 h before each imaging session; during neuronal tract tracing, 100 mM $MnCl_2$ was administered into the substantia nigra 2 wks after 6-OHDA lesioning.

MRI was performed 24 h after the lesion, followed by weekly MRI over 7 weeks. Rats were anesthetized with 1.5% isofluorane and placed prone in a stereotaxic holder with brain centered in a 72/25 mm volume transmit/surface receive coil ensemble. Body core temperature was maintained at 37 °C with warm air flow over the rat. A pressure transducer was used to monitor the respiration cycle. MRI was performed on a 21-cm horizontal bore 7 Tesla scanner operating on an Avance platform (Bruker Biospin).

Three mutually perpendicular slice images through the brain were acquired as scout images. Fourteen contiguous 1-mm-thick axial images (slice number 6–7 centered at the bregma) of the brain were acquired using a fast spin echo (FSE) sequence [matrix 2562, NA = 8, echoes = 8, TR/TE = 3,500/14.15 ms, field of view (FOV) = 3.2 cm]; an identical set of FSE images with T1 weighting (TR/TE = 355/10.25 ms) was also acquired. To obtain quantitative T2 values, T2 weighted axial images (TR/TE = 3,500/20 ms, 8 echoes, FOV = 3.2 cm, matrix 1282) were acquired. A 2D multi-slice look-locker sequence (6) with 20 point samples along the inversion recovery curve was used to calculate T1 (TE/TR = 2.2/104 ms, flip angle = 250, FOV = 3.2 cm, matrix 128, slice thickness = 1 mm, inversion interval = 400 ms).

Quantitative T1 and T2 maps were calculated using custom written software in MATLAB (Mathworks) taking into account the perturbation caused by flip angle in determining T1.

In Vivo Experiments—Monkeys. ***Preparation of gadolinium-DTPA.*** Clinical grade gadolinium-DTPA (Berlex) was used in all infusions. The gadolinium-DTPA was diluted in PBS solution to a 1 mM concentration.

Convective co-infusion of growth factors and gadolinium-DTPA. Six (2 controls, 2 treated with Dll4, and 2 treated with Ang2) adult primates (*Macaca mulatta*) underwent convection enhanced delivery (CED) co-infusions to the right striatum. Each animal received 120 μL aCSF, 0.4 mg/mL Dll4, or 0.2 mg/mL Ang2 in PBS with BSA carrier (0.1%) and 1 mM gadolinium-DTPA. The animals were sedated, intubated, and placed under isoflurane general endotracheal anesthesia. The animals' temperature, heart rate, oxygen saturation, electrocardiographic responses, and end-tidal partial pressure of carbon dioxide were continually monitored. The head of each animal was then secured in a stereotactic frame (model 9-YSTI; Crist Instrument). Using sterile technique, a midline skin incision was made from the anterior to the posterior aspect of the vertex of the skull and self-retaining retractors were used to expose the underlying bone. An 8-mm-burr hole was placed in the calvarium over the stereotactically determined entry point above the target area and the underlying dura mater was incised. A 22-gauge fused silica outer guide cannula (outer diameter 0.027 in, inner diameter 0.02 in) was stereotactically placed through the dural opening along the target trajectory to a level 1.5 cm above the desired striatal target. The guide cannula was secured to the calvarium with methylmethacrylate. The inner cannula (outer diameter 0.014 in, inner diameter 0.006 in), after being connected to the infusion apparatus, was placed through the outer guide cannula to the target.

To distribute infusate to the striatum using CED, we used a noncompliant delivery system that is gastight with no dead volume that has been described previously. A Harvard syringe pump (PHD 2000; Harvard Apparatus) was used to generate continuous pressure throughout the infusion procedure. During infusion, pressure was transmitted from the pump to a glass, gastight, infusate-filled Hamilton syringe (250 μL total volume) that was connected to PE50 thick-walled polyethylene tubing (outer diameter 0.050 in, inner diameter 0.023 in; Plastics One). The tubing was connected to the distal end of the inner infusion cannula, and the tip was placed directly into striatum. Infusions were carried out at 0.5 μL/min. After the infusion was complete, the cannulas were removed and the animals were euthanized. During the euthanizing process the brain was flushed with heparinized saline and 4% paraformaldehyde solutions before being removed. A 1.5-cm-thick bilateral coronal slab was removed from the fixed brain, which included both the ipsilateral and contralateral infused hemispheres and was immediately snap-frozen for later immunohistochemistry assays.

Imaging of factors and gadolinium-DTPA distribution. After placement of the infusion cannula, coronal T1-weighted MR images were obtained to determine the precise location of the infusion cannulas. Once cannula placement was confirmed, infusions were started and T1-weighted MR images were obtained in 3 planes (sagittal, axial, and coronal; slice thickness 1 mm, 0 mm spacing) using a 3 Tesla MRI-scanner. Images were obtained at ≈10- to 20-min intervals until the infusions were complete.

Cell numbers and vascular effects were assessed by immunohistochemistry using several (typically 6) coronal sections taken between +21 mm and +31 mm relative to Ear Bar Zero (EBZ).

Reagents. We used the following reagents and antibodies: FGF2 (233-FB), mouse Dll4 (1389-D4), fibronectin (1030-FN), human

angiopoietin-2 (623-AN), from R&D Systems; JAK Inhibitor I (420099), from Calbiochem; polyornithine (P-3655), insulin (I9278) from Sigma; BrdU (84447723) from Boehringer; Fluorogold from Fluorochrome, LLC; Alexa-Fluor-conjugated secondary antibodies and Alexa-conjugated Phalloidin (A12379) from Invitrogen; ECL reagents (34080) from Pierce; polyacrylamide gradient gels from Invitrogen; HRP-conjugated secondary antibodies from Jackson Immunoresearch; DAPI (D-8417) from Sigma, and general chemicals from Sigma. For immunohistochemical staining, we used antibodies against the following markers: nestin (MAB353; Chemicon), Tuj1 (MMS-435P; Covance), GFAP (z0334) and CD31 (M0823) from Dako; CNPase (MAB326; Chemicon), BrdU (H5903; Accurate), Sox2 (MAB2018; R&D Systems); Hes3 (25393), Tie2 (sc-324), Tie2 (sc-31266), STAT3 (482), pSer727-STAT3 (8001-R), pTyr705-STAT3 (7993), Akt (5298), Ang1 (sc-6319), Ang2 (sc-7015), from Santa Cruz Biotechnology; tyrosine hydroxylase (P80101 and P40101; Pel-Freez); RECA-1 (MCA 970GA) from Serotec; pTie2 (AF2720) from R&D Systems; pSer473-Akt (92715), pThr308-Akt (9275), pSer2448-mTOR (29715), p38 (9212), pThr180/Tyr-182-p38 (9211), from Cell Signaling; α-tubulin, Tie2 (AF313; R&D Systems), pTie2 (AF2720; R&D Systems) and (T-6074; Sigma); RECA-1 (MCA 970GA) from Serotec; Magnevist from Berlex Imaging.

Quantitations. The number of animals per experimental group is given in the text (*Results* section). Typically, 4–10 adult rats were used per group; 2 adult animals per group were used in the primate experiments. $BrdU^+$ and Hes3-positive cell numbers in rats were counted in several (typically 6) 30-μm-thick sections. SVZ and striatal sections were collected between bregma +1.70 and −0.40 mm; substantia nigra sections were collected between bregma −4.80 and −6.30 mm. Hippocampal sections were collected between bregma −3.14 and −5.3 mm. Blood vessels counts in adult rats were also made between bregma +1.70 and −0.40 mm (the images shown correspond to bregma +1.56). When the brains were sectioned, sectioning started at bregma 2.20 mm and sequential sections were collected on glass slides and frozen. This allowed us to approximate the corresponding location of each section in the anterior-posterior axis. The exact location corresponding to the sections used was determined by assessing the morphology of the SVZ, DG, the third ventricle, and the third ventricle/aqueduct. TH^+ signal in the striatum was quantified from digital immunohistochemistry images for TH; the data are represented as TH signal in the ipsilateral (to the treatment) side expressed as a percentage of the contralateral value to control for variability among immunohistochemistry sessions. TH in the substantia nigra is scored as the number of cells per field of view (with a 10× objective) that express TH (this field of view contains the entire area of the substantia nigra in the coronal sections used); the numbers presented are for cells that are double-positive for both TH and fluorogold to count TH^+ cell bodies in the substantia nigra that have uninterrupted projections to the striatum (the site of fluorogold injection). Immunohistochemical co-localizations were scored in the areas described above—all images obtained were confocal stacks, and the images shown are projections of confocal stack, 3D representations from confocal stacks, or series of single images along the z axis.

3D image reconstruction. We used the Volocity 3D imaging software by Improvision (http://www.improvision.com/products/volocity/) and Zeiss Axiovision (http://www.zeiss.com) software on confocal z-stacks.

Statistical analysis. Results shown are the mean ± SEM. Asterisks identify experimental groups that were significantly different (P value < 0.05) from control groups by the Student's t test (Microsoft Excel), where applicable. The P values shown are within the value allowed after Bonferroni correction. In Fig. 6*E* (Rotometry dose curves), the asterisks represent statistical significance as determined by 2-way ANOVA analysis (by the GraphPad Prism software). Table S1 is presented with the P values for each experiment.

1. Johe KK, Hazel TG, Muller T, Dugich-Djordjevic MM, McKay RD (1996) Single factors direct the differentiation of stem cells from the fetal and adult central nervous system. *Genes Dev* 10:3129–3140.
2. Saharinen P, *et al.* (2008) Angiopoietins assemble distinct Tie2 signalling complexes in endothelial cell-cell and cell-matrix contacts. *Nat Cell Biol* 10:527–537.
3. Fukuhara S, *et al.* (2008) Differential function of Tie2 at cell-cell contacts and cell-substratum contacts regulated by angiopoietin-1. *Nat Cell Biol* 10:513–526.
4. Lee JH, Koretsky AP (2004) Manganese enhanced magnetic resonance imaging. *Curr Pharm Biotechnol* 5:529–537.
5. Kuo YT, Herlihy AH, So PW, Bell JD (2006) Manganese-enhanced magnetic resonance imaging (MEMRI) without compromise of the blood-brain barrier detects hypothalamic neuronal activity in vivo. *NMR Biomed* 19:1028–1034.
6. Chuang KH, Koretsky A (2006) Improved neuronal tract tracing using manganese enhanced magnetic resonance imaging with fast T(1) mapping. *Magn Reson Med* 55:604–611.

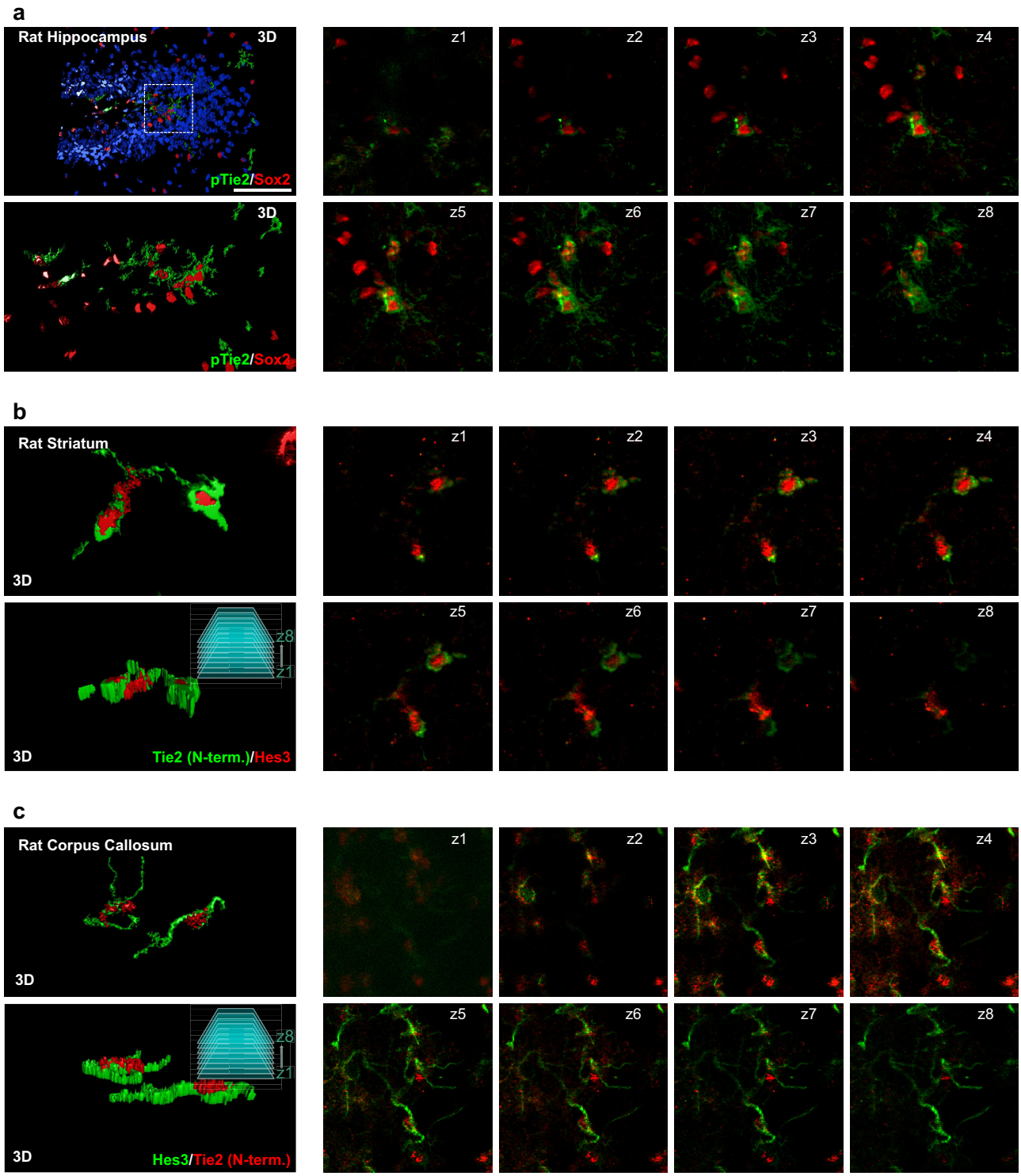

Fig. S1. Tie2-positive precursors in the adult rat brain co-express Sox2 and Hes3. (*a*) Example of pTie2/Sox2 co-staining in the adult rat hippocampus. (*b*) Example of Tie2/Hes3 co-staining in the adult rat striatum. (*c*) Example of Hes3/Tie2 co-staining in the adult rat corpus callosum. 3D, 3D software reconstructions from confocal z stacks; z1–z8, series of single plane, 1-μm-thickness images from a confocal z stack; the axis of the z series is represented graphically in the lower, 3D reconstruction (Scale bars, 50 μm).

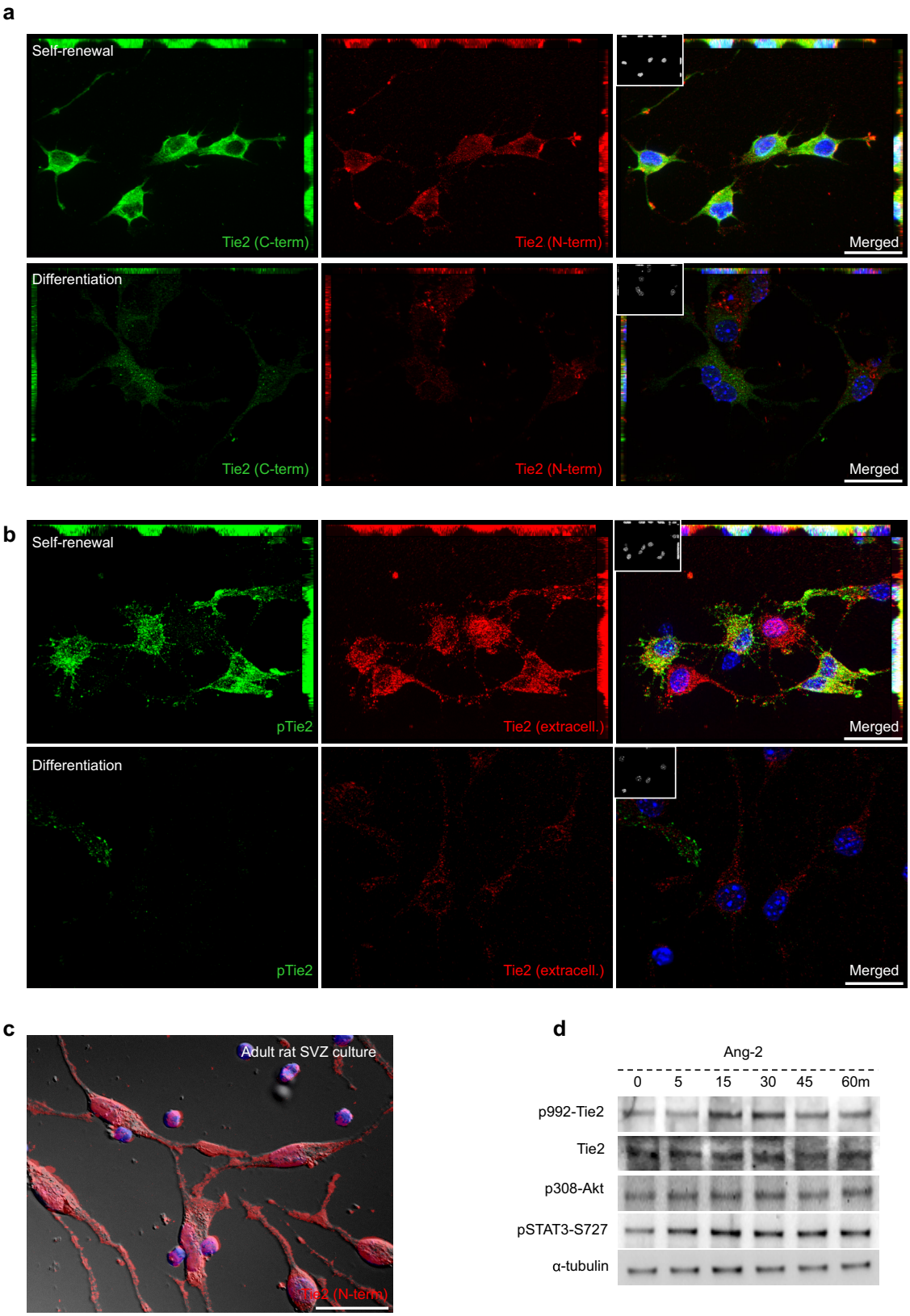

Fig. S2. Neural stem cells in vitro express the Tie2 receptor. (*a* and *b*) Fetal NSC cultures express the angiopoietin receptor Tie2 (4 antibodies were used against the N, C, terminus of Tie2 as well as against an extracellular domain and the phosphorylated form of Tie2); Tie2 expression is lost following differentiation by a 1-week FGF2 withdrawal. (*c*) Adult rat SVZ neural stem cell cultures express Tie2. (*d*) Ang-2 treatment of fetal NSC cultures induces the phosphorylation of Tie2 and STAT3-S727. Western blot data from time-course experiments are shown (Scale bars, 50 μm).

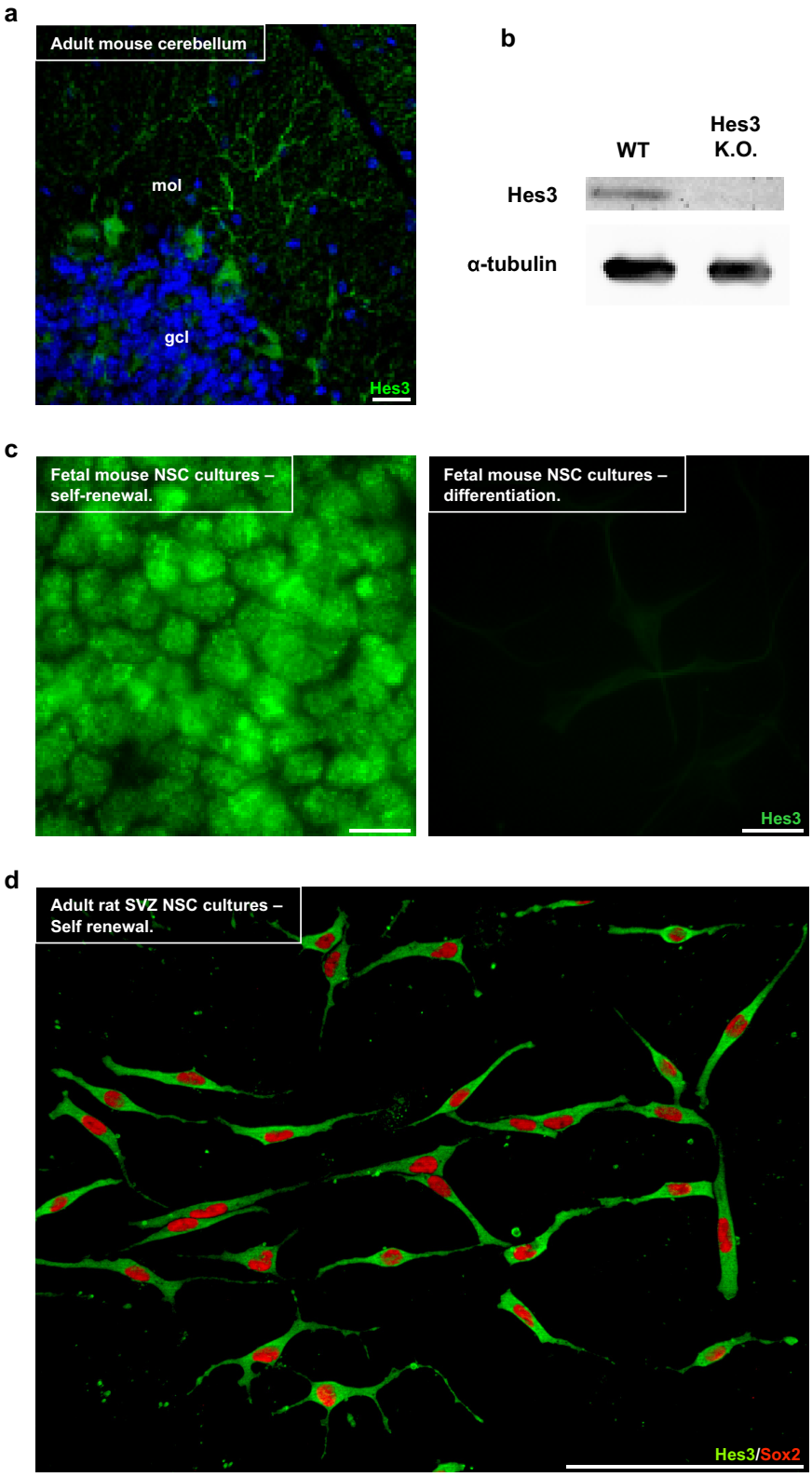

Fig. S3. Neural stem cells in vitro express Hes3. (*a*) Purkinje cells in the adult mouse cerebellum are recognized by the anti-Hes3 antibody (mol, molecular layer; gcl, granule cell layer). (*b*) The anti-Hes3 antibody identifies a band in the wild-type but not Hes3 null cerebellar protein extracts. (*c*) Fetal mouse NSC cultures express Hes3; Hes3 expression is lost following a 1-week differentiation period (by FGF2 withdrawal). (*d*) Adult rat SVZ neural stem cell cultures co-express Hes3 and Sox2 (Scale bars, 50 μm).

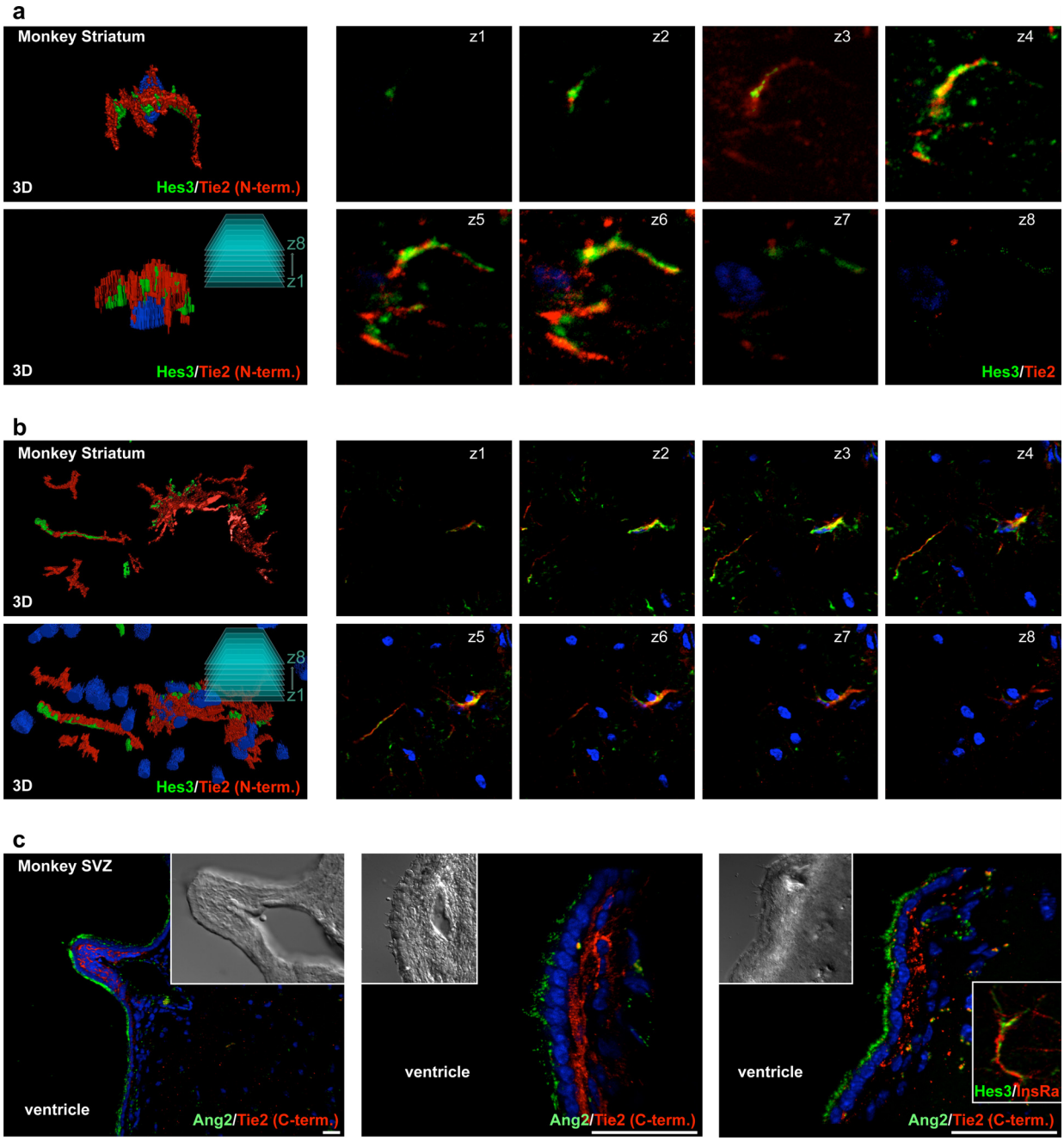

Fig. S4. Hes3-positive precursors in the adult monkey brain co-express InsRa and Tie2. (*a* and *b*) Example of Hes3/Tie2 co-staining in the adult monkey striatum. (*c*) Additional examples of foci described in Fig. 1*F*. 3D, 3D software reconstructions from confocal z stacks; z1–z8, series of single plane, 1-μm-thickness images from a confocal z stack; the axis of the z series is represented graphically in the lower, 3D reconstruction; inset, Hes3/InsRa double-positive cell in the striatum (Scale bars, 50 μm).

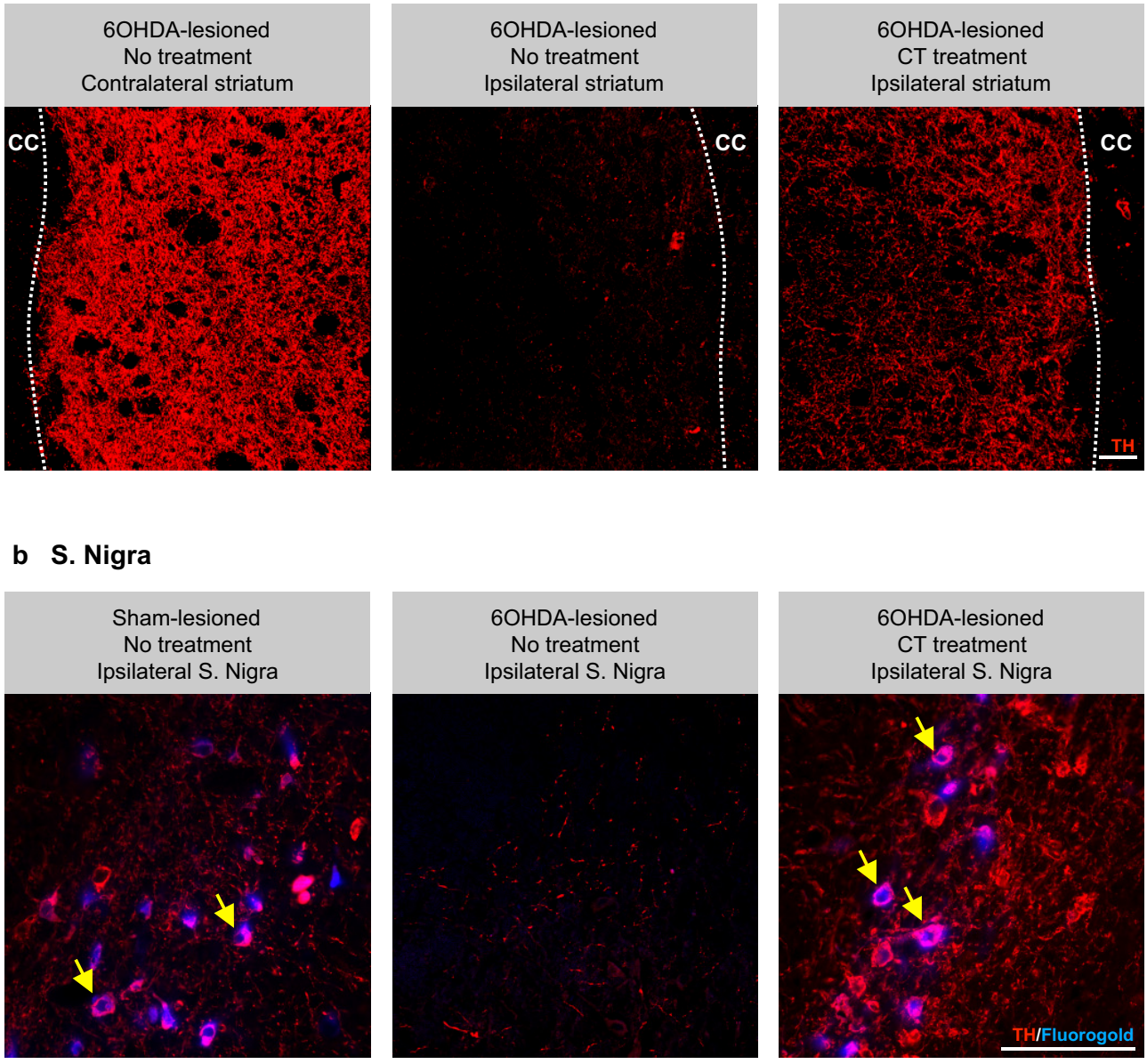

Fig. S5. Injured dopamine neurons are protected from death by single treatments with angiogenic factors. (*a*) Single intracerebroventricular injections of Dll4, Ang2, and CT result in an increase in TH^+ signal in the lesioned rat striatum (representative images are shown; the dotted lines represent the boundary between the lateral striatum and corpus callosum; ''CC'', corpus callosum). (*b*) When administered 2 weeks after a 6-OHDA lesion, the same treatments also rescue TH^+ cell bodies in the substantia nigra (assessed 13 weeks after treatment). Dopamine neurons were retrogradely labeled by fluorogold injections in the striatum, 1 week before euthanization; data are numbers of $Fluorogold^+/TH^+$ cell bodies in the substantia nigra as a % control. (Arrows point to examples of $TH^+/Fluorogold^+$ cell bodies; Scale bars, 50 μm.)

Table S1. Significance (*P*) values

Fig.	*P* Value	Description
1*E*	Dll4 from control: 0.0069	Tie2 OD
	Dll4 from control: 0.00088	InsRa OD
1*F*	Contra; Dll4 from control: 0.0025	Foci (Contra)
	Ipsi; Dll4 from control: 4.03×10^{-5}	Foci (Ipsi)
2*A*	SVZ: Dll4, 0.03890; Ang2, 0.01973; CT, 2×10^{-5}	BrdU + cell # in adult rat
2*B*	SVZ: Dll4, 3.6×10^{-5}; Ang2, 6.34×10^{-6}; CT, 2.12×10^{-8}	Hes3 cell # in adult rat
2*h*	Striatum: 0.000457, 0.001602, 5.26×10^{-5}	Hes3 in adult rat
	S.Nigra: 0.002309, 0.001491, 0.001303	
2*I*	Dll4: 0.01205101	Hes3 in adult monkey
	Ang2: 0.0049	
3*B*	Object #: Dll4, 0.037103; Ang2, 0.004074	Vessel number; rat
3*C*	Object area: Ang2, 0.003068	Vessel size; rat
3*D*	Object area: Dll4 vs. Ang2, 0.00030922	Vascular Size, Area; monkey [$n = 2$ monkeys]
4*A*	Ang2, 0.006849; Dll4, 0.001291; CT, 0.002526	TH signal in STR
4*B*	Ang2, 0.001603; Dll4, 0.007546; CT, 0.0037	TH/FG in S. Nigra
4*C*	Dll4 vs. control: 0.0012	Behavior; 2-way ANOVA
	Ang2 vs. control: <0.0001	
	CT vs. control: <0.0001	

Statistical significance (*P* values) corresponding to the figures presented are shown. Results from *t* test analyses are shown for Figs. 1*E* and 4*B* [The *P* values are within limits applied by the Bonferroni correction]. For the rotometry curves in Fig. 4*C*, *P* values from two-way ANOVA are shown.